NASA TM-84241

NASA Technical Memorandum 84241

NASA-TM-84241 19820017386

Barriers and Dispersal Surfaces in Minimum-Time Interception

N. Rajan and M. D. Ardema

LIBRARY COPY

MAY 2 9 1982

LANGLEY RESEARCH CENTER
LIBRARY, NASA
HAMPTON, VIRGINIA

May 1982

NASA
National Aeronautics and
Space Administration

NASA Technical Memorandum 84241

Barriers and Dispersal Surfaces in Minimum-Time Interception

N. Rajan
M. D. Ardema, Ames Research Center, Moffett Field, California

National Aeronautics and
Space Administration

Ames Research Center
Moffett Field, California 94035

N81-24161 #

Barriers and Dispersal Surfaces in Minimum-Time Interception[1]

N. RAJAN[2] AND M. D. ARDEMA[3]

Abstract. Dispersal points and points on the Barrier are located for a class of pursuit-evasion and interception problems. These points are determined by constructing cross sections of the isochrones and hence obtaining the Barrier, Dispersal, and control-level surfaces. The method is illustrated through examples from minimum-time interception of a target moving in a straight line in a horizontal plane.

Key Words. Barriers, minimum-time interception, aircraft flight paths optimization.

1. Introduction

The area of optimizing aircraft maneuvers is quite complex and has received extensive attention. In Ref. 1, minimum-time turns to a line or a point in the plane are investigated when the final velocity and heading are specified. The destination point or line is taken far away from the starting point so that the aircraft has sufficient time to accelerate to maximum speed in all cases. The solution is obtained by integrating the optimal trajectory backward from termination. The assumption of long-duration makes the extremals

[1]The authors are indebted to F. Neuman, M. Sidar, J. Shinar, H. Erzberger, and G. Leitmann for their comments. The first author wishes to acknowledge the financial support of the National Research Council.

[2]NRC Research Associate, Ames Research Center, NASA, Moffett Field, California.

[3]Research Assistant to the Director, Ames Research Center, NASA, Moffett Field, California.

a one-parameter family. The two-boundary-value problem of choosing the extremal that satisfies the given initial conditions is thus simplified. Under the restriction of long-duration maneuvers, time-scale separation of turning and acceleration is possible, and singular perturbation approaches (Refs. 2, 3) have been successful in obtaining feedback approximations. However, short- and intermediate-duration maneuvers do not show up in these analyses. Aircraft maneuvers in a tail-chase pursuit-evasion game have been investigated in Ref. 4, employing a differential dynamic programming algorithm. The numerical examples show tail-chase maneuvers of short duration.

In this paper, minimum-time interception of a target moving in a horizontal plane is analyzed as a one-player differential game (Ref. 5). The game solution gives the interceptor's strategy in a feedback form. It first addresses the question whether the target can be captured from all initial positions relative to the interceptor. If not, the Barrier, a closed-surface bounding the initial positions from which capture is possible, is constructed. Even if capture is possible for all initial states, a Barrier may exist, but in this case it is an open surface across which the game value, here the time-to-capture, is discontinuous, and the nature of the optimal trajectories changes drastically.

The game solution maps the controls as a function of the state within the capture region. This is done by backward integration of the state and adjoint equations from termination. The integration has to be stopped at surfaces where the adjoints are discontinuous; such surfaces are called singular surfaces (Ref. 5). One of the most frequently encountered singular surfaces is the Dispersal surface. Along such a surface, one player can choose between two distinct strategies and still obtain the same payoff. Constructing the Barrier and Dispersal surfaces is therefore an inherent part of a differential game solution.

In a game with four or five state variables, visualization of the Barrier and Dispersal surfaces is difficult. This is circumvented by constructing the cross sections of these surfaces with two or more of the state variables held constant. A stack of such cross sections then describes the surfaces. This paper describes a method of computing the locations of points on these cross sections. Although minimum-time interception in the plane is used as an example, the extension of the method to pursuit-evasion in the plane, which is straightforward, is also outlined.

The analysis uses a device first developed in Refs. 6-8. The motion of the interceptor and the target are described in a coordinate system whose origin is fixed at the interceptor's terminal position, and the x-axis is along the terminal line of sight. The equations that describe the interceptor's optimal motion backward in time from termination do not contain any reference to the target motion. They can be integrated independently to give extremal trajectory maps (ETM) (Ref. 6). Using this concept, cross sections of the Barrier were constructed by direct iteration of the terminal Mach numbers of the pursuer and evader in Refs. 6-8. In this paper, constant initial Mach number and relative heading cross sections of the isochrones (constant-time loci) are drawn. At Dispersal points (DP), two branches of an isochrone intersect. An isochrone ends if capture becomes impossible for the given time-to-go. The endpoints thus fall on a Barrier cross section.

The interception problem is formulated and the necessary conditions for optimality are derived in Section 2. Extremal trajectory maps are shown for a given initial interceptor speed. The method of constructing a global solution is described in Section 3. Isochrone cross sections for interception are depicted, and some interception encounters in the plane are shown. The extension of the method to pursuit-evasion is outlined.

2. Problem Statement

2.1 Formulation. The motion of the target in the plane is described in terms of its coordinates $[x_T(t), y_T(t)]$ in any conventient set of axes. Since the motion is prescribed a priori, the target motion is a function of time alone. In the same coordinate frame, the interceptor's motion is goverened by

$$\dot{x}_I = M_I \cos\beta_I, \tag{1}$$

$$\dot{y}_I = M_I \sin\beta_I, \tag{2}$$

$$\dot{M}_I = A(M_I)\pi - B(M_I) - C(M_I)\omega^2 \tag{3}$$

and

$$\dot{\beta}_I = \omega a(M_I)/M_I, \tag{4}$$

subject to the state-variable constraint,

$$M_I \varepsilon [\underline{M}, \overline{M}], \tag{5}$$

with the throttle setting π and the bank control ω chosen such that

$$\pi \varepsilon [0, 1] \quad \text{and} \quad \omega \varepsilon [-1,1].$$

The above description of the aircraft's motion is the same as that given in Ref. 6. Briefly, β_I is the interceptor's heading measured from the x-axis (counterclockwise positive); M_I is the Mach number; A represents the maximum thrust, B is the zero bank drag, C is the lift-induced drag at the maximum bank, and a is the angular acceleration. The target is considered to have been intercepted when brought within a line of sight (LOS) distance of R of the interceptor. This is,

$$[x_T(t_f) - x_I(t_f)]^2 + [y_T(t_f) - y_I(t_f)]^2 = R^2 \tag{6}$$

at the instant of interception t_f, the interceptor must be reducing the separation distance or

$$\dot{r} = M_T(t_f)\cos\beta_T(t_f) - M_I(t_f)\cos\beta_I(t_f) < 0 \tag{7}$$

to effect capture. Where interception occurs, the payoff is the time taken to capture the target. The performance index, augmented by the terminal constraint (6), is

$$J_a = \nu[(x_T(t_f) - x_I(t_f))^2 + (y_T(t_f) - y_I(t_f))^2 - R^2] + \int_o^{t_f} dt. \tag{8}$$

As in the analyses of pursuit-evasion, (Refs. 6-8) the coordinate axes, to which the above equations refer, are selected such that the origin coincides with the interceptor's terminal position, and the x-axis is along the terminal line of sight (Fig. 1). The position and orientation of the axes thus change from engagement to engagement. As is shown below, this choice of axes makes the trajectory equations and the expressions for the optimal controls for the interceptor independent of the target motion. The analysis is simplified and leads very naturally to the method of locating Dispersal points, which is developed later.

2.2 The Necessary Conditions. The Hamiltonian for the minimum-time interception problem is written as

$$H = 1 + \lambda_x \dot{x}_I + \lambda_y \dot{y}_I + (\lambda_M + \mu)\dot{M}_I + \lambda_\beta \dot{\beta}_I, \tag{9}$$

where λ_x, λ_y, are the position adjoints; λ_M and λ_β are the velocity and heading adjoints; and the multiplier μ accounts for the first-order state-variable (Ref. 9) constraint on the interceptor's Mach number. It satisfies the Kuhn-Tucker conditions,

$$\mu \begin{cases} <0 & \text{if } M_I = \underline{M}, \\ = 0 & \text{if } \underline{M} < M_I < \overline{M}, \\ >0 & \text{if } M_I = \overline{M}. \end{cases} \tag{10}$$

From the Euler-Lagrange equations and the transversality conditions plus the particular choice of coordinate axes mentioned above, it can be shown that the adjoints satisfy (Appendix)

$$\lambda_x = -2\nu R, \tag{11}$$

$$\lambda_y \equiv 0, \tag{12}$$

and

$$\lambda_\beta = -2\nu R y_I. \tag{13}$$

The vanishing of the Hamiltonian at t_f gives the value of the multiplier ν as

$$\nu = (2R(M_{If}\cos\beta_{If} - M_{Tf}\cos\beta_{Tf}))^{-1} > 0; \tag{14}$$

ν is positive because the target's velocity relative to the interceptor has a negative component along the line of sight at the endpoint.

Because H does not involve time explicitly, a first integral of motion is given by (Appendix)

$$\min_{(\pi,\omega)} H = -2\nu R\, M_{Tf}\cos\beta_{Tf}. \tag{15}$$

When the normalized velocity adjoint ρ_M and the multiplier $\bar{\mu}$ are defined, repectively, as

$$\rho_M \overset{\Delta}{=} \lambda_M / 2\nu R \tag{16}$$

and

$$\bar{\mu} \triangleq \mu/2\nu R, \tag{17}$$

and by using (11)-(13) in (9), then (15) becomes

$$\min_{(\pi,\omega)} H_I = -M_{If}\cos\beta_{If}, \tag{18}$$

where

$$H_I \triangleq (\rho_M+\bar{\mu})\dot{M}_I-\dot{x}_I-y_I\dot{\beta}_I. \tag{19}$$

Minimizing H_I with respect to (π,ω) subject to the constraints $\pi\varepsilon[0,1]$, $\omega\varepsilon[-1,1]$ yields the following expression for the optimal controls:

$$\pi = 1$$

$$\omega = \mathrm{sat}(-ay_I/(2CM_I(\rho_M+\bar{\mu}))) \text{ for } \rho_M+\bar{\mu}<0 \tag{20}$$

and

$$\pi = 0$$

$$\omega = \mathrm{sign}(y_I) \text{ for } \rho_M+\bar{\mu}>0. \tag{21}$$

The normalized velocity adjoint appearing in the above expressions satisfies the differential equation

$$\dot{\rho}_M = \cos\beta_I-(\rho_M+\bar{\mu})(-dA/dM_I-\omega^2 dc/dM_I)+ \tag{22}$$

$$\omega y_I(da/dM_I-a/M_I)/M_I.$$

Note that the canonical equations (1), -(4), and (22), together with the controls (20) and (21) contain no reference to the target motion; the same type of "open-loop optimality" found in pursuit-evasion is obtained here.

Backward integration of the extremals depends only on the terminal-velocity vector of the interceptor and is independent of target motion. Thus a map of the extremals may be generated integrating backward from the origin; this is called the extremal trajectory map (ETM) in Refs. 6 and 7.

2.3 Extremal Trajectory Maps. Each extremal in an ETM may be considered to be specified by a triplet of values (β_f, M_f, τ_f), where β_f and M_f are the terminal heading and Mach number, and $\tau_f (= t_f - t_0)$ is the time-to-go. For any given pair of values for β_f and τ_f, it is possible to select an M_f value, through a one-dimensional search, such that the Mach number at τ_f matches a given value M_o. The ETMs used here are collections of extremals that start out from a given initial Mach number. They can be combined with a target/pursuer/evader's ETM to yield a global solution for any given encounter. For this, apart from the triplet (β_f, M_f, τ_f), the initial coordinates (x,y) and heading β are needed. The behavior of the bank and throttle along the extremals determines the values of τ_f for which isochrones need be drawn (Section 3).

The trajectories in the plane for $\tau_f = 10$ sec are shown in Fig. 2a. The variation of Mach number, heading and bank with retro time is shown in Figs. 2b - 2d. For $\beta_f = 0°$, the aircraft flies in a straight line at full throttle, accelerating from Mach 0.9 to Mach 1.02. The extremal with $\beta_f = 0.33°$ starts out at half-bank and gradually straightens out to near-level flight. The angle of turn $\Delta\beta = 23°$, and the terminal Mach number is slightly above unity. On the next extremal, the bank decreases from unit magnitude at start to below 0.1 at termination; $\Delta\beta = 45°$, and the average turn rate is about half the maximum instantaneous at Mach 0.9. As β_f increases beyond 0.85°, the bank saturation instant moves closer to termination, till at $\beta_f = 15°$, the entire trajectory is flown at full bank.

These trajectories represent different trade-offs between turn and speed. However, their initial points would not appear on the cross section of the unit bank control surface taken with the initial Mach number equal to 0.9. Between $\beta_f = 15°$ and 77°, the extremals are constant control arcs; both bank and throttle are full throughout. The Mach number time-history is identical for all extremals in this range of β_f and is hence a single curve in Fig. 2b. The turn angle $\Delta\beta = 109°$, or the average turn rate = 10.9°/sec. Between 77° and 90°, the extremals start out with the throttle closed and switch to full throttle sometime later; this switching instant moves toward t_f with increasing β_f till, at 90°, the extremals terminate with zero throttle. The region between $\beta_f = 90°$ and 100°, shows throttle switches from zero to full and back to zero; for $\beta_f = 100°$, at $\tau = 9.5$(0 to 1) and 6.6(1 to 0) sec, respectively. Beyond $\beta_f = 100°$, the extremals are all flown at zero throttle, full bank; the Mach number variation is independent of β_f (Fig. 2b).

The 140° and 160° extremals show switchings in bank (Fig. 2c) where they intersect the x-axis. Such maneuvers reduce the turn angle; the net effect is to brake down while heading in the same direction. Such a maneuver is resorted to when the target is close behind and heading in the same direction. In Fig. 2a, the extremals for $\beta_f = 140°$ and 160° appear to intersect. However, the heading angles at the point of intersection are different, as can be seen from Fig. 2c.

Bank and throttle switching disappear as τ_f increases beyond 25 sec. The behavior of the extremals with increasing τ_f becomes more uniform and can be summarized as follows: as τ_f increases, the values of β_f for the same $\Delta\beta$ decrease steadily (for $\tau_f = 60$ sec, $\beta_f = 0.0005°$ for $\Delta\beta = 200°$); all extremals have partial bank segments and are full-throttle throughout for the

initial Mach number of 0.9. As τ_f increases further, the terminal Mach number hits the speed boundary. The extremals then consist of an unconstrained (maximum Mach number constraint) arc accelerating up to $\overline{M}$, a circular arc at $\overline{M}$, then a straight dash at $\overline{M}$ along the negative x-axis. Such extremals, called cruise arcs, are similar to those discussed in Ref. 1. However, the use of these extremals to locate Dispersal points depends only on a decoupling coordinate transformation approach being possible; it is discussed next.

3. Construction of a Feedback Solution

A feedback solution to interception or pursuit-evasion must give the control strategies and the value at any point in the state-space. One way of presenting the solution is to draw the boundaries of the regions within which the strategies are constant. Where a control varies continuously over a range, as does the bank here, the surfaces at which the control attains specified values are mapped. Since these boundaries and surfaces are in a four or five dimensional state-space, they can be visualized by cross sectioning. They are sectioned by keeping the initial Mach numbers of the interceptor and target, or of the pursuer and evader, and the initial relative heading, constant. The cross sections are then plotted relative to the interceptor/pursuer and become curves in the plane of the encounter.

The control-level surfaces, Barrier Points (BP), and Dispersal Points are all located by drawing cross sections of the isochrones (the optimal parts of the isochrones are isocost). The control-level surface links the points on the isochrone at which the controls take on a specified set of values. Dispersal Points are located at the intersections of different branches of the same isochrone. Where the isochrone cross sections are not closed, their

endpoints are on a Barrier cross section. Such a section separates two families of isochrones. The construction of the isochrone sections for interception is described next.

3.1 Isochrones for Interception. Assume that the interceptor and target ETMs are as shown in Figs. 3a and 3b, respectively. The interceptor's map comprises extremals generated for a specified time to go with the terminal heading β_f as a parameter. For each extremal in the map, the initial Mach number is M_{Io}; the initial heading measured relative to the terminal line of sight equals β_{Io}. The target's initial Mach number is given as M_{To}. Since the target's motion is prescribed, the target's terminal Mach number M_{Tf} and the angle of turn $\Delta\beta_T$ at τ_f are known. Although the target's motion in the plane is fixed, its heading relative to the terminal line of sight β_{Tf} varies with the different paths flown by the interceptor. The target's ETM consists of the target's path in the plane rotated through several different values of β_{Tf} (the term ETM is used only as a convenience).

If the relative heading of the isochrone section being constructed is β_o, then the initial heading of the target measured from the terminal LOS must be equal to $\beta_{Io}+\beta_o$. Since the target's angle of turn is $\Delta\beta_T$, its terminal heading equals $\beta_{Io}+\beta_o-\Delta\beta_T$. In the construction of a locus point (Fig. 3c), the interceptor's extremal is first laid off as IA. The terminal LOS is AB. Since the target's heading relative to AB is known, it can be laid off as shown, TB. The point T is the point on the locus, provided the terminal LOS rate is negative; that is

$$M_{Tf}\cos(\beta_{Io}+\beta_o-\Delta\beta_T)-M_{If}\cos\beta_f<0.$$

Different values of β_f give other points on the locus. Points of interest on the extremals, for example bank saturation, throttle, and bank

switching, also get mapped on the isochrone locus section. For a section with a different relative heading, these points are rotated by the difference in β_o. The method plots all candidate points for the isochrone. This is true because extremals for all possible values of β_f are generated. Some of the resulting points are not optimal because there are other constant-time loci points for a lower time-to-go overlapping them. A Dispersal point occurs if two extremals with different values of β_f pass through the same point in reduced space. Neither extremal is globally optimal beyond the DP.

The location of Dispersal and Barrier points and the construction of isochrones are explained by examples.

3.2 Examples. Figure 4a shows some isochrone section for an interceptor initial Mach number of 0.9 and a relative heading of 135°. The points A_1 to A_4 are those for which $\beta_f = 0°$; the interceptor just flies straight ahead at full throttle to meet the target. To the right of these points, the interceptor banks to the right, and the terminal heading β_f is positive. For all the sections, β_f increases in the direction C to B. The sections do not extend beyond the points B and C because the "reachability" condition is not met; thus, the envelope of these points delineates the $\beta_o = 135°$, $M_{Io} = 0.9$ section of the Barrier (Ref. 5). However, since the interceptor has a maximum Mach number capability of 1.6, it can capture the target, given sufficient time. This can be seen from Fig 4b where the 30 sec locus is also shown. Across B_3, there is a discontinuity in the time-to-go. From B_3 to P, the time-to-go is 30 sec. The PQD_1 portion of the constant-time locus for $t_f = 30$ sec is nonoptimal and does not form part of any isochrone. All points on PQD_1 are conjugate points; however, only D_1 and P actually appear on the isochrone sections. This suggests that not all values of β_f lead to extremals that are globally optimal for a given value of β_o;

there are points for $\tau_f = 20$ sec which fall between the origin and the 15-sec locus and are hence obviously non-optimal globally.

Figure 4c shows a more complete picture of the isochrone sections with τ_f ranging from 5 to 60 sec. The 60-sec locus is the first one that is closed. Even for an initial range of 2 km, 60 sec is the globally optimal time-to-capture because of the unfavorable initial conditions. The target has a higher initial speed and its direction is away from the interceptor. The interceptor turns left and accelerates to Mach 1.2 with its terminal heading almost aligned with the final LOS. This encounter starting from P is depicted in real space in Fig. 5. The locus shows a Dispersal point at D. Extremals with two different values of β_f pass through D; they are shown in the plane in Fig. 6.

In Fig. 7, an isochrone section with $\beta_o = 0°$ and $\tau_f = 20$ sec is shown. The Dispersal point at D_1 is one along a Dispersal surface where the interceptor flies symmetric paths starting with either a left or a right turn; the values of β_f at D_1 are $\pm 116°$. The encounter at D_1 is shown in Fig. 8. Another interesting kind of Dispersal point occurs at D_2 in Fig. 7. Two branches of the locus, one with β_f decreasing toward 90° and the other with β_f increasing, intersect at D_2. The encounter at D_2 is shown in Fig. 9.

The additional computational effort to map the feedback solution, given the ETMs, is relatively small. Moreover the logic of determining the Barrier and Dispersal Points can be automated. The generation of the ETM data storage is a straightforward, though tedious process; once done, however, the data are common to any interception/pursuit evasion problem in which the given aircraft is a participant. The method of constructing maps of strategies and isochrones can serve as a useful tool for design, displays, training, and testing of sub-optimal approximations. The extension of the method to interception and

pursuit-evasion in three dimensions is, in principle, straightforward. If the aircraft is modeled based on the energy-state approximation, with the specific energy replacing the Mach number as a variable, a similar structure is obtained. The extension of the method to pursuit-evasion is outlined.

3.3 Pursuit-Evasion. The above method of constructing isochrone sections can be employed for an actively evading target. The cross sectioning would be done for fixed initial Mach numbers and relative heading for the pursuer and evader. The evader's ETM would be constructed in exactly the same way as the pursuer's, with β_f, τ_f, as parameters and M_f iterated till the initial Mach number is matched. For each point on a constant-time locus, the evader's ETM would be searched for the extremal that has an initial heading equal to $\beta_o+\beta_{Io}$. The "reachability" condition would be checked for the extremal. This search for the extremal in the evader's ETM is independent of the search for the M_f value that generates it. Other features of the method are the same as for interception.

4. Conclusions

A method of locating Barrier and Dispersal points for a class of minimum-time interception and pursuit-evasion problems has been developed. The method obtains these points, which are an essential part of the game solution, by drawing cross sections of the isochrones. Examples are shown for minimum-time interception in a horizontal plane. The method can be extended to solve pursuit-evasion between two aircraft in the plane and in three dimensions.

Appendix

The differential equations for the adjoints are

$$\dot{\lambda}_x = 0, \tag{A1}$$

$$\dot{\lambda}_y = 0, \tag{A2}$$

$$\dot{\lambda}_M = -\lambda_x \cos\beta_I - \lambda_y \sin\beta_I - (\lambda_M + \mu)(\pi dA/dM - dB/dM - \omega^2 dC/dM) \tag{A3}$$

$$+ \dot{\lambda}_\beta \omega (a/M - da/dM)/M,$$

and

$$\dot{\lambda}_\beta = \lambda_x \dot{y}_I - \lambda_y \dot{x}_I. \tag{A4}$$

For the choice of coordinate axes shown in Fig. 1, the transversality conditions give

$$\lambda_x(t_f) = -2\nu R, \tag{A5}$$

$$\lambda_y(t_f) = \lambda_\beta(t_f) = \lambda_M(t_f) = 0, \tag{A6}$$

and

$$H(t_f) = -2\nu R M_{Tf} \cos\beta_{Tf}. \tag{A7}$$

In (A7), M_{Tf} and β_{Tf} are the target's terminal Mach number and heading. Equations (A1), (A2), and (A4), together with the end conditions (A5) and (A6), yield (11) - (13). The substitution of (A5) in (A7) leads to (14).

References

1. BRYSON, Jr., A. E., and PARSONS, M. G. Constant Altitude Minimum-Time Turns to a Line and to a Point for a Supersonic Aircraft with a Constraint on Maximum Velocity, SUDAAR No. 437, Stanford University, Nov. 1971.

2. CALISE, A. J., Singular Perturbation Techniques for On-Line Optimal Flight Path Control, Paper 79-1621, AIAA Atmospheric Flight Mechanics Conference, Boulder, Colo., Aug. 6-8, 1979.

3. FARBER, N., and SHINAR, J., An Approximate Feedback Solution of a Variable Speed Non-Linear Pursuit-Evasion Game between Two Airplanes in a Horizontal Plane, Paper 80-1597, AIAA Atmospheric Flight Mechanics Conference, Danvers, Mass., Aug. 11-13, 1980.

4. JARMARK, B. S. A., MERZ, A. W. and BREAKWELL, J. V., The Variable-Speed Tail-Chase Aerial Combat Problem, AIAA Journal of Guidance and Control, Vol. 4, No. 3, May-June 1981, pp. 323-328.

5. ISAACS, R., Differential Games, John Wiley & Sons, New York, 1965.

6. RAJAN, N., PRASAD, U. R., and RAO, N. J., Pursuit-Evasion of Two Aircraft in a Horizontal Plane, AIAA Journal of Guidance and Control, Vol. 3, No. 3, May-June 1980, pp. 261-267.

7. PRASAD, U. R., RAJAN, N. and RAO, N. J., Planar Pursuit-Evasion with Variable Speeds, Part 1, Extremal Trajectory Maps, Journal of Optimization Theory and Applications, Vol. 33, No. 3, Mar. 1981, pp. 401-418.

8. RAJAN, N., PRASAD, U. R., and RAO, N. J., Planar Pursuit-Evasion with Variable Speeds, Part 2, Barrier Sections, Journal of Optimization Theory and Applications, Vol. 33, No. 3, Mar. 1981, pp. 419-432.

9. BRYSON, Jr., A. E., and HO, Y. C., Applied Optimal Control, John Wiley, 1975 (revised).

List of Figure Captions

Fig. 1. Choice of corrdinate axes.

Fig. 2. Extremal trajectory map: (a) paths in the plane; (b) Mach number time history; (c) heading time-history; (d) bank control time-history.

Fig. 3. Construction of a point on a constant-time locus.

Fig. 4. Constant-time loci in reduced space: (a) loci for 5, 10, 15, and 20 secs; (b) additional 30-sec locus with nonoptimal segments; (c) Barrier and Dispersal points.

Fig. 5. Long-duration encounter starting close-in.

Fig. 6 Interceptor paths for a DP on the 1-min locus.

Fig. 7. A 20 sec locus with 2 DPs.

Fig. 8. Interceptor path with bank switching.

Fig. 9. The two possible paths from the Dispersal Point D_2.

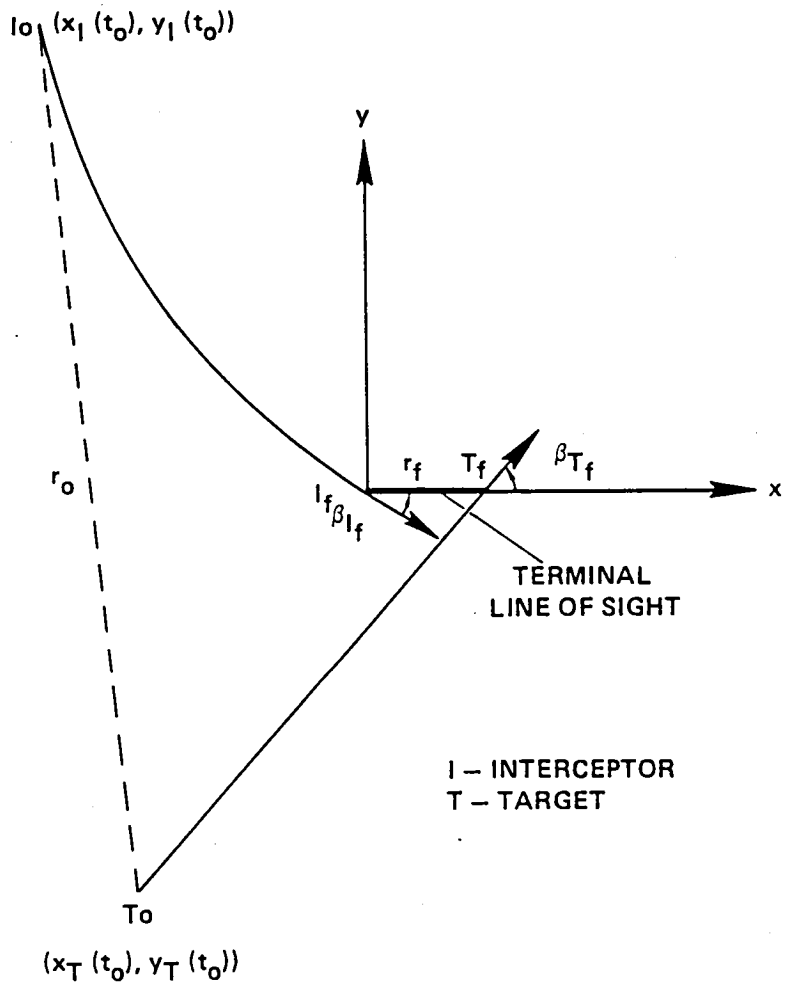
Io
$(x_I(t_o), y_I(t_o))$
y
r_o
r_f
T_f
βT_f
x
I_f
βI_f
TERMINAL
LINE OF SIGHT
I – INTERCEPTOR
T – TARGET
To
$(x_T(t_o), y_T(t_o))$

Fig. 1

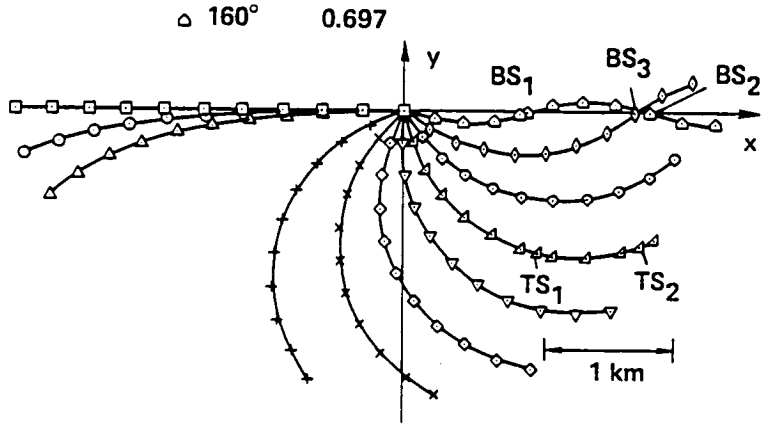

BS_1, BS_2, BS_3 – BANK SWITCH POINTS
TS_1, TS_2 – THROTTLE SWITCH POINTS

Fig. 2a

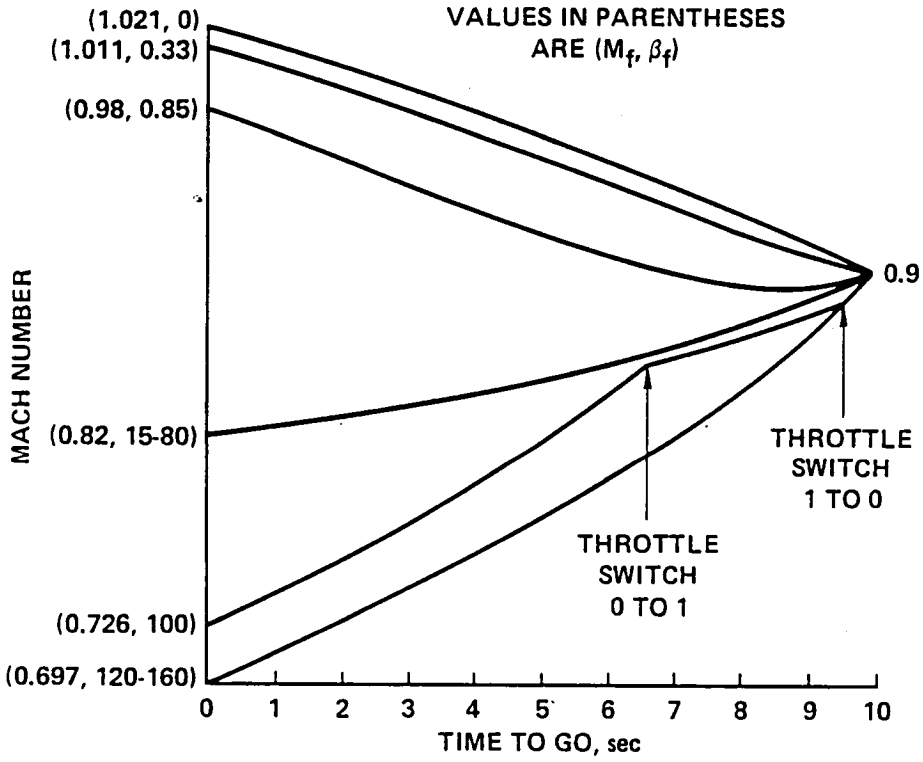
VALUES IN PARENTHESES
ARE (M_f, β_f)
(1.021, 0)
(1.011, 0.33)
(0.98, 0.85)
(0.82, 15-80)
(0.726, 100)
(0.697, 120-160)
MACH NUMBER
0.9
THROTTLE
SWITCH
1 TO 0
THROTTLE
SWITCH
0 TO 1
0
1
2
3
4
5
6
7
8
9
10
TIME TO GO, sec

Fig. 2b

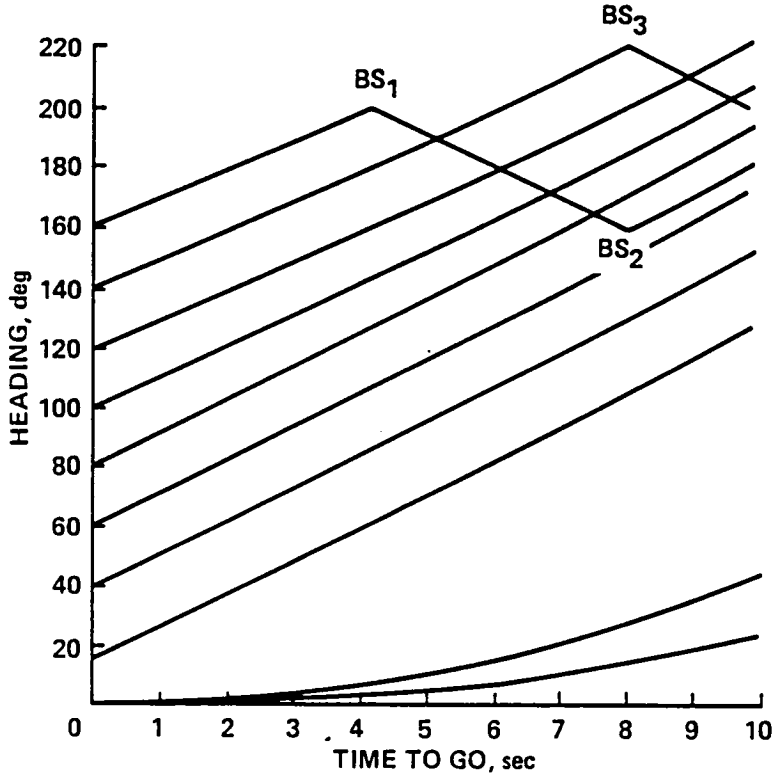

BS_1, BS_2, BS_3 – BANK SWITCH POINTS

Fig. 2c

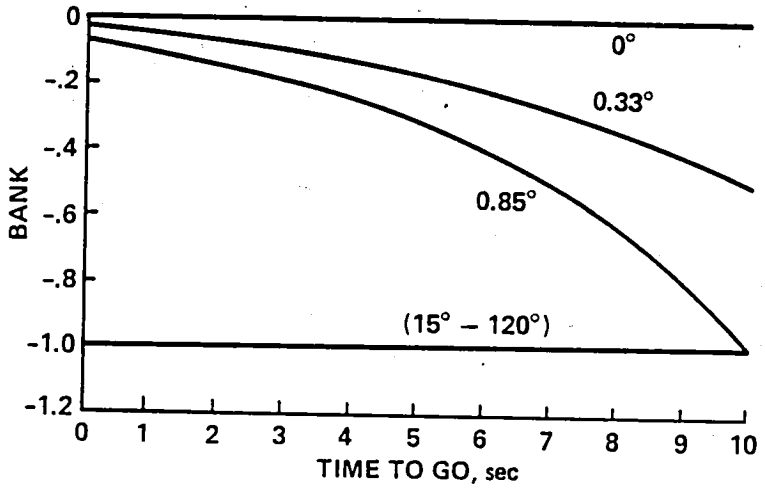

(β_f MARKED ALONG THE CURVE)

Fig. 2d

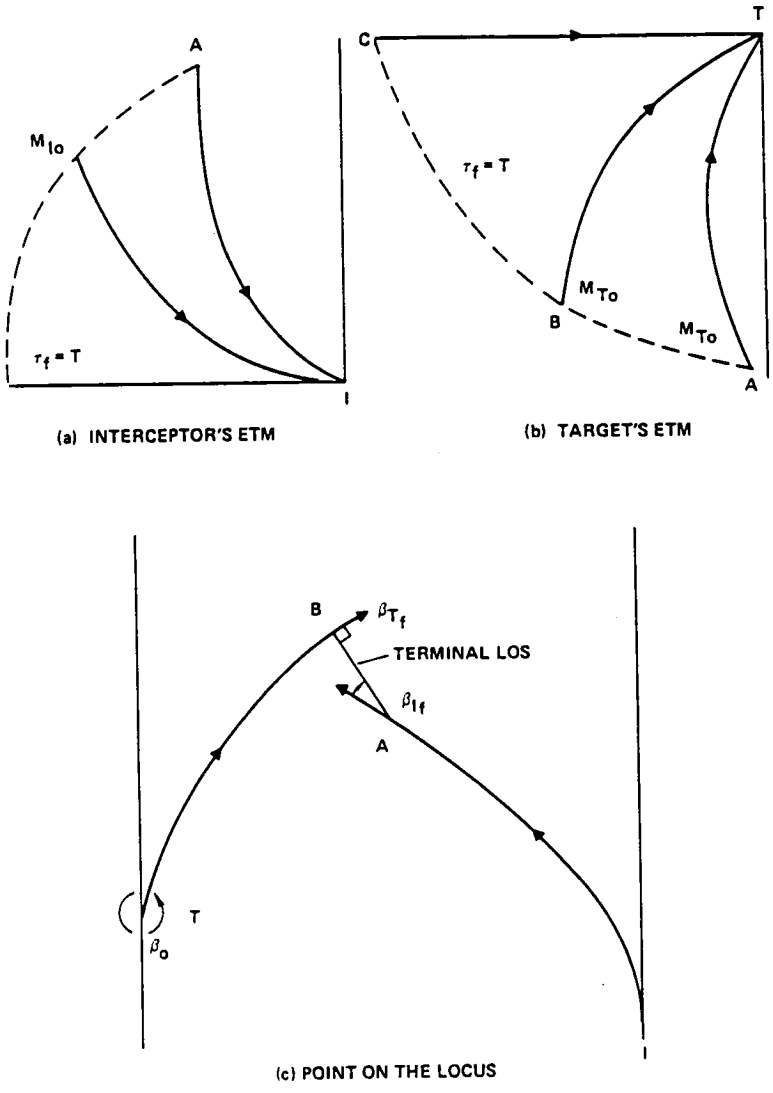

(a) INTERCEPTOR'S ETM

(b) TARGET'S ETM

(c) POINT ON THE LOCUS

Fig. 3

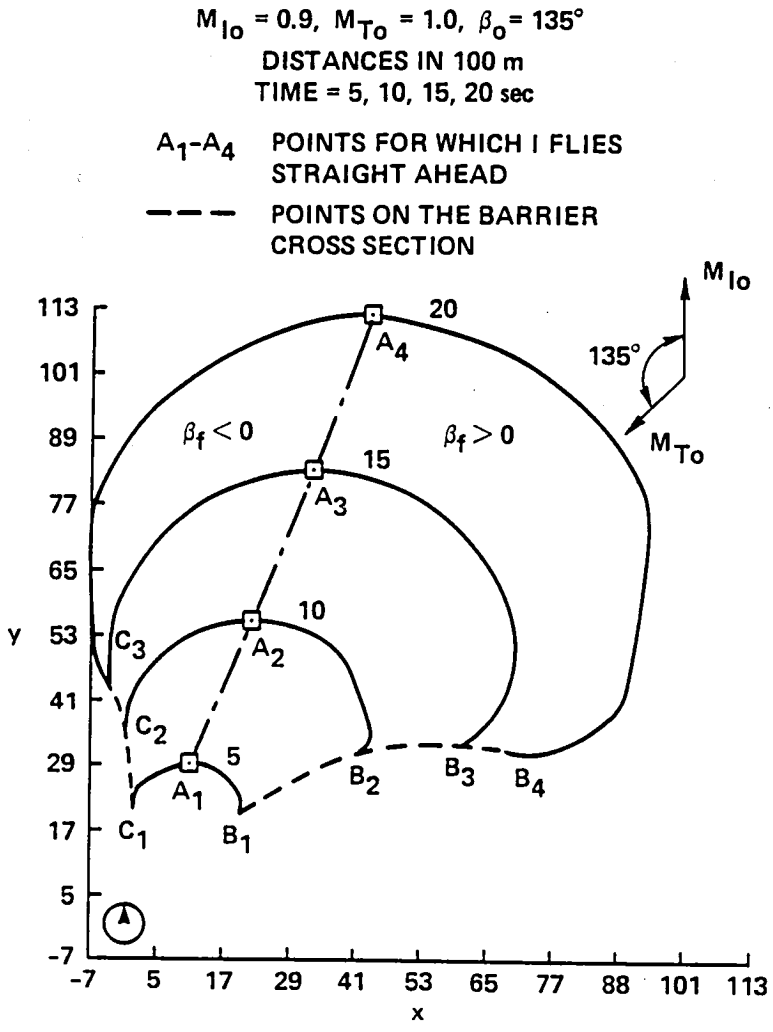
M_{Io} = 0.9, M_{To} = 1.0, β_o = 135°
DISTANCES IN 100 m
TIME = 5, 10, 15, 20 sec
A_1-A_4 POINTS FOR WHICH I FLIES STRAIGHT AHEAD
POINTS ON THE BARRIER CROSS SECTION
M_{Io}
135°
M_{To}
$\beta_f < 0$
$\beta_f > 0$
20
15
10
5
A_1
A_2
A_3
A_4
B_1
B_2
B_3
B_4
C_1
C_2
C_3
y
x
113
101
89
77
65
53
41
29
17
5
-7
-7
5
17
29
41
53
65
77
88
101
113

Fig. 4a

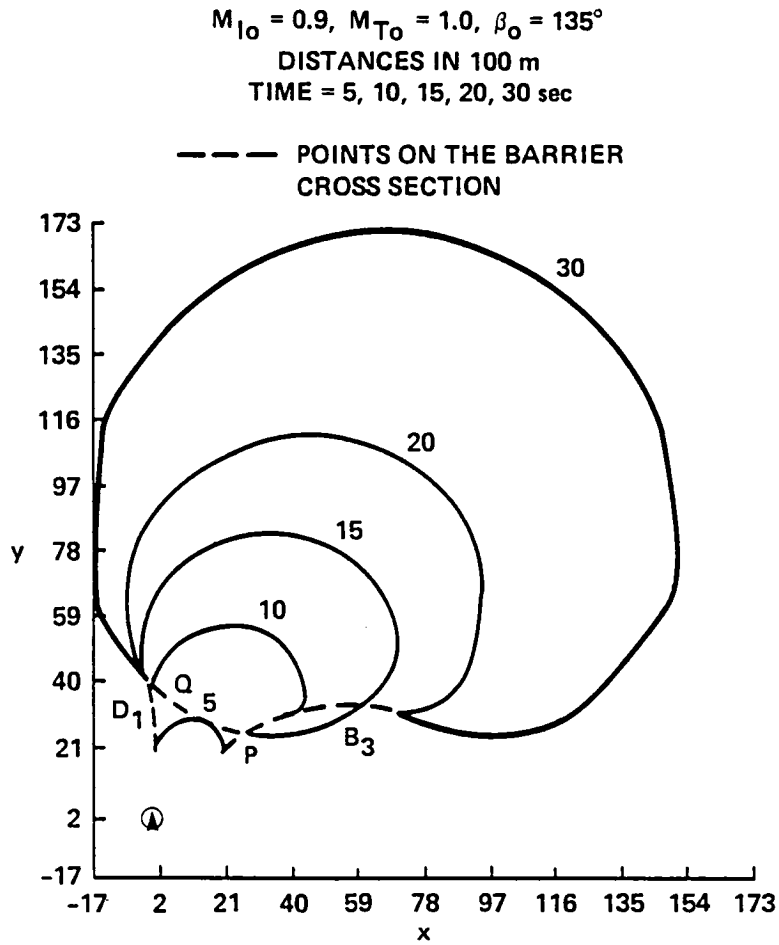
M_{Io} = 0.9, M_{To} = 1.0, β_o = 135°
DISTANCES IN 100 m
TIME = 5, 10, 15, 20, 30 sec
POINTS ON THE BARRIER CROSS SECTION
173
154
135
116
97
y 78
59
40
21
2
-17
-17 2 21 40 59 78 97 116 135 154 173
x
30
20
15
10
5
Q
D_1
P
B_3

Fig. 4b

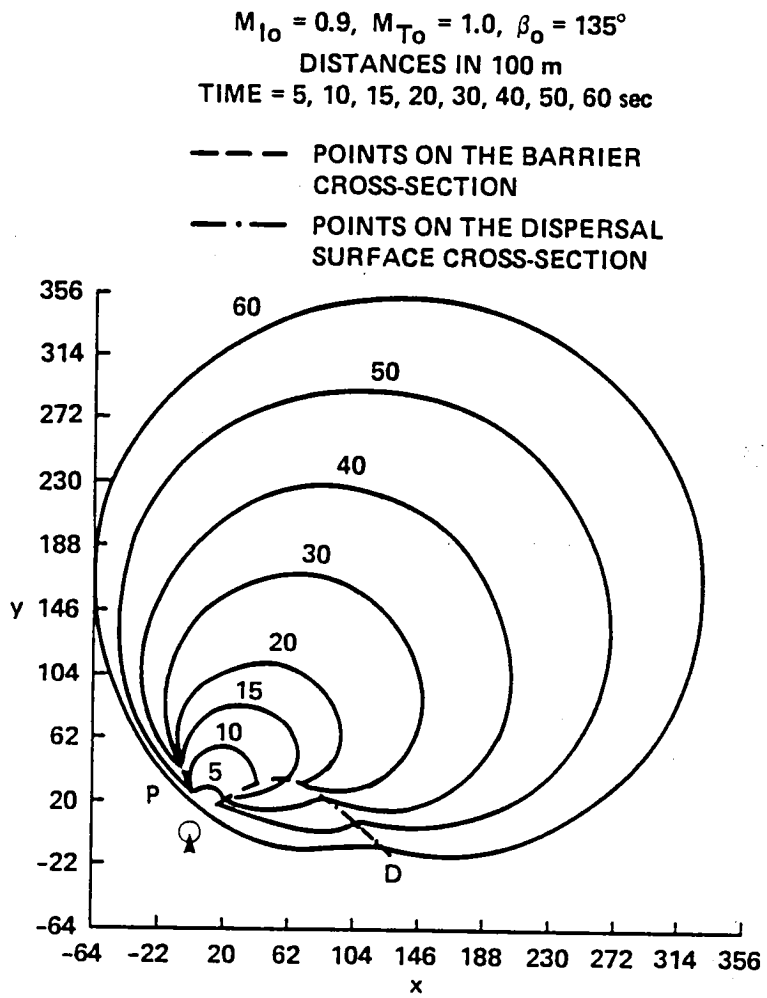
M_{Io} = 0.9, M_{To} = 1.0, β_o = 135°
DISTANCES IN 100 m
TIME = 5, 10, 15, 20, 30, 40, 50, 60 sec
POINTS ON THE BARRIER CROSS-SECTION
POINTS ON THE DISPERSAL SURFACE CROSS-SECTION
356
314
272
230
188
y 146
104
62
20
-22
-64
-64 -22 20 62 104 146 188 230 272 314 356
x
60
50
40
30
20
15
10
5
P
D

Fig. 4c

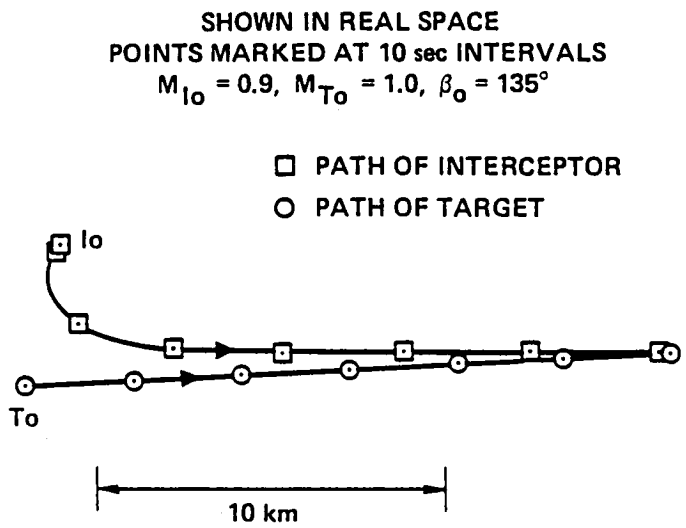
SHOWN IN REAL SPACE
POINTS MARKED AT 10 sec INTERVALS
$M_{Io} = 0.9$, $M_{To} = 1.0$, $\beta_o = 135°$
PATH OF INTERCEPTOR
PATH OF TARGET
Io
To
10 km

Fig. 5

SHOWN IN REAL SPACE
POINTS MARKED AT 10 sec INTERVALS

□ INTERCEPTOR PATH – β_f = -4.1 e - 4° M_f = 1.209
○ TARGET PATH – β_o = 135° τ_f = 60 sec
△ INTERCEPTOR PATH – β_f = 4.3 e - 4° M_f = 1.21

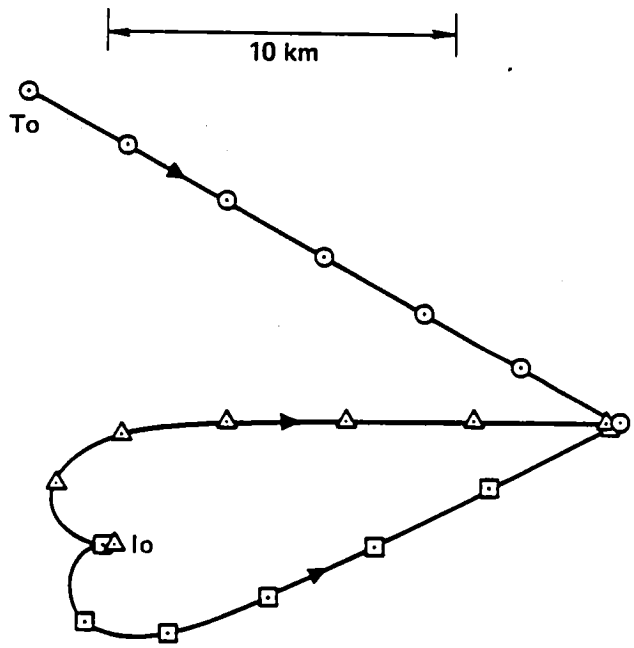

Fig. 6

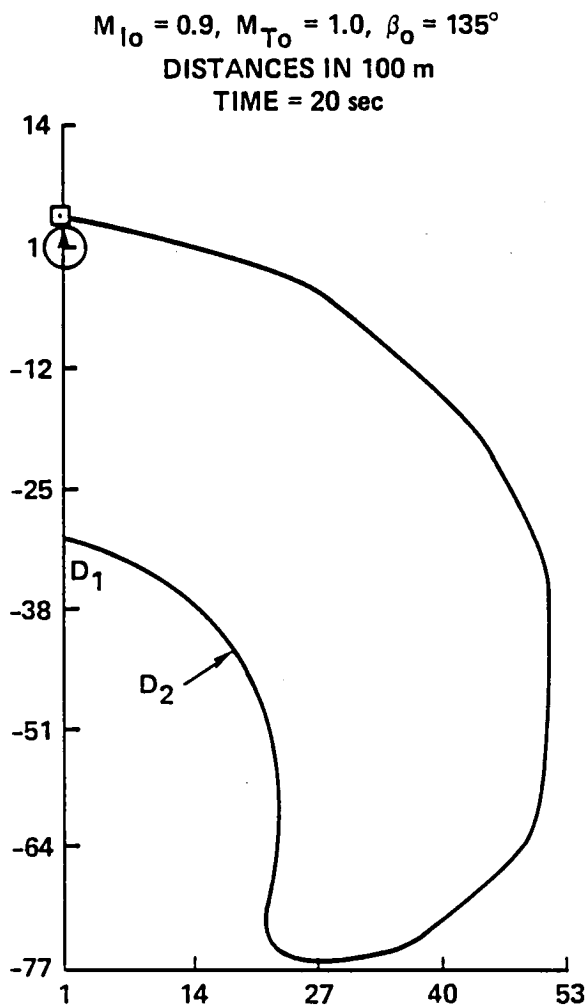
M_{Io} = 0.9, M_{To} = 1.0, β_o = 135°
DISTANCES IN 100 m
TIME = 20 sec
14
1
-12
-25
-38
-51
-64
-77
1
14
27
40
53
D_1
D_2

Fig. 7

SHOWN IN REAL SPACE
POINTS MARKED AT 1 sec INTERVALS

□ INTERCEPTOR PATH – $\beta_f = 116°$ $M_f = 0.576$

○ TARGET PATH – $\beta_o = 0°$ $\tau_f = 20$ sec

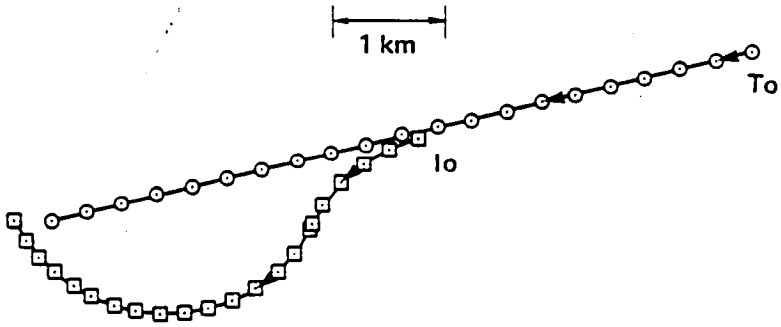

Fig. 8

SHOWN IN REAL SPACE
POINTS MARKED AT 1 sec INTERVALS

□ INTERCEPTOR PATH – $\beta_f = 99.5°$ $M_f = 0.576$
○ TARGET PATH – $\beta_o = 0°$ $\tau_f = 20$ sec
△ INTERCEPTOR PATH – $\beta_f = 83.5°$ $M_f = 0.8$

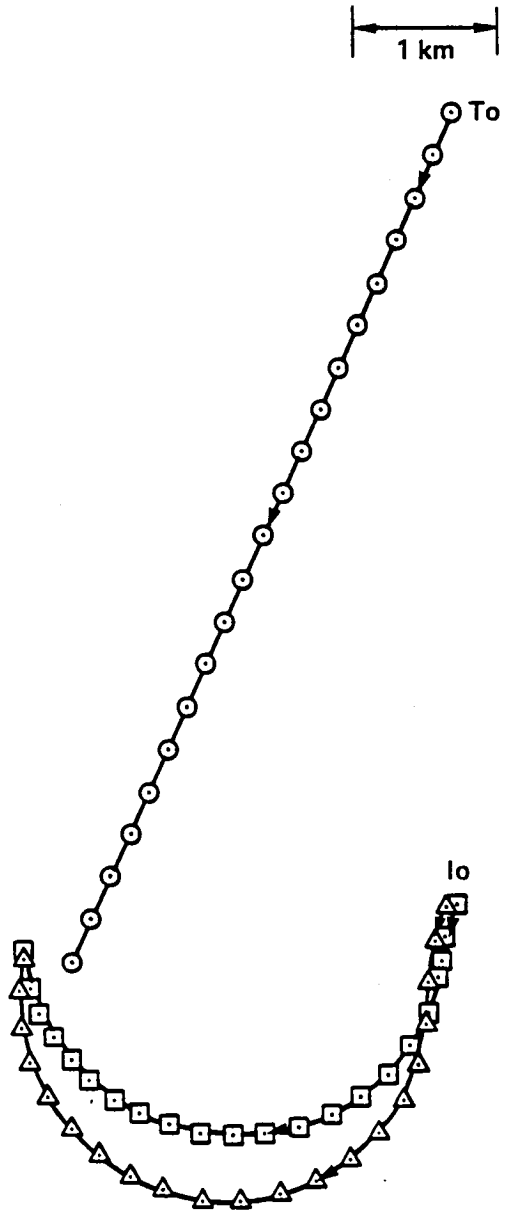

Fig. 9

1. Report No.	2. Government Accession No.	3. Recipient's Catalog No.
NASA TM 84241		

4. Title and Subtitle	5. Report Date
Barriers and Dispersal Surfaces in Minimum-Time Interception	May 1982
	6. Performing Organization Code
7. Author(s)	8. Performing Organization Report No.
N. Rajan and M. D. Ardema	A-8912
9. Performing Organization Name and Address	10. Work Unit No.
NASA Ames Research Center Moffett Field, Calif. 94035	T-5896
	11. Contract or Grant No.
12. Sponsoring Agency Name and Address	13. Type of Report and Period Covered
National Aeronautics and Space Administration Washington, D. C. 20546	Technical Memorandum
	14. Sponsoring Agency Code
	307-02-01

15. Supplementary Notes

Point of Contact: N. Rajan, M/S 210-9, Moffett Field, CA. 94035.
(415) 965-5433, FTS 448-965-5433

16. Abstract

Dispersal points and points on the Barrier are located for a class of pursuit-evasion and interception problems. These points are determined by constructing cross sections of the isochrones and hence obtaining the Barrier, Dispersal, and control-level surfaces. The method is illustrated through examples from minimum-time interception of a target moving in a straight line in a horizontal plane.

17. Key Words (Suggested by Author(s))	18. Distribution Statement
Barriers, minimum-time interception Aircraft flight paths optimization	Unlimited Subject Category 08

19. Security Classif. (of this report)	20. Security Classif. (of this page)	21. No. of Pages	22. Price*
Unclassified	Unclassified	32	A03

*For sale by the National Technical Information Service, Springfield, Virginia 22161

LANGLEY RESEARCH CENTER
3 1176 00504 0259